

Topographic-Isostatic Reductions in Satellite Gravity Gradiometry Based on a Generalized Condensation Model

B. Heck, F. Wild

Geodetic Institute, University of Karlsruhe, Englerstr 7, D-76128 Karlsruhe, Germany
e-mail: heck@gik.uni-karlsruhe.de; Fax: +49-721-608-6808

Abstract. In satellite gravity gradiometry, the gravitational signals from the Earth's topography and its isostatic compensation still exist in the gravity gradients observed along the satellite orbit. Due to the high-frequency behaviour of the combined topographic-isostatic effect, downward continuation of the gravitational signal from satellite height to sea level is rather difficult, requiring some mathematical method of regularization. On the other hand, the complete calculation of topographic-isostatic effects according to, say, the Airy-Heiskanen isostatic model is too laborious for the practical evaluation of gravity gradiometry data. In this paper, another approach is proposed, which is based on a generalized condensation model corresponding to Helmert's first condensation model; here the condensed masses are assumed to be situated on a surface at a constant depth D below the geoid. The respective formulae representing the effects of the topographic and condensation masses on the vertical gravity gradient (V_{π}) at satellite level are derived. A simulation based on the JGP95E rock-equivalent terrain model proves that the order of magnitude of both topographic and condensation effects is about 10 E.U. The magnitude of the combined topographic-condensation effect is much smaller, amounting to 0.6 E.U. and 0.06 E.U. for Helmert's first and second condensation model, respectively.

Keywords. Satellite gravity gradiometry, topographic reductions, Helmert's condensation models

1 Introduction

The Earth's topographic masses and its isostatic balance masses produce gravitational signals in external space, which will also be visible in satellite

gravity gradiometry (SGG) observations, e.g. in the planned GOCE mission. Similar to terrestrial applications, it should be advantageous to reduce the effects of the topographic-isostatic masses in satellite gradiometry by some kind of remove-restore technique in order to produce a smooth field which can be downward continued more easily. The conventional procedure applied in terrestrial gravity field modelling relies on the computation of the gravitational effects of rectangular prisms – based on a detailed gridding of the topographical-isostatic masses (Tsoulis 1999; Kuhn 2003). Unfortunately the numerical effort is extremely high in this case.

In this paper, it is proposed to reduce these calculations to the evaluation of two-dimensional surface integrals. Assuming a constant topographic density, the respective volume integral can be analytically integrated over the height parameter, providing a two-dimensional spherical integral. On the other hand, taking Helmert's idea of condensation (see e.g. Heck 2003), a simple isostatic model can be constructed which behaves similarly to the Airy-Heiskanen isostatic model. The respective formulae for the evaluation of the second radial derivative of the topographic and isostatic potential constituents are derived in detail, and the numerical properties are outlined with the aid of a simulation.

2 Topographic Reductions of SGG Data

The gravitational potential of the topographical masses between sea level, approximated by the "geoidal sphere" Σ_g (radius R), and the Earth's topographical surface S is described by Newton's integral. Assuming a constant density ρ of the topographical masses and decomposing the triple integral into a two-dimensional spherical integral over σ and a one-dimensional integral over the radial parameter ξ results in

$$V_i(Q) = G \cdot \rho \cdot \iint_{\sigma} \left[\int_{R}^{r'} \frac{\xi^2}{\ell} d\xi \right] \cdot d\sigma \quad (1)$$

$$\ell := \sqrt{r^2 + \xi^2 - 2r\xi \cdot \cos\psi} \quad (2)$$

where r is the radius of the computation point Q , ψ the angle between the geocentric radius of Q and the variable integration point P' on S (see Figure 1), r' the geocentric radius of P' , and G is the gravitational constant.

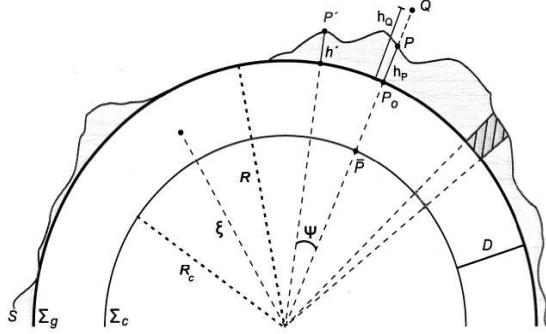


Figure 1. Geometry of the topography and the condensation model in spherical approximation

In Figure 1, $r = R + h_Q$ is the geocentric radius of the computation point Q , $r' = R + h'$ is the geocentric radius of the variable integration point $P' \in S$, and $r_p = R + h_p$ the radius of the point P below Q at the intersection with the topographical surface S .

In Appendix A, the following expression for the second vertical (radial) derivative of the topographical potential V is proved:

$$\frac{\partial^2 V_i(Q)}{\partial r^2} = \frac{2}{r} \cdot \frac{\partial V_i(Q)}{\partial r} - \frac{2}{r^2} \cdot V_i(Q) + \frac{G\rho}{2r^2} \iint_{\sigma} \left[\frac{3\xi^3}{\ell} + \frac{\xi^3(r^2 - \xi^2)}{\ell^3} \right]_{\xi=R}^{\xi=r'} \cdot d\sigma \quad (3)$$

Formulae for $V_i(Q)$ and its first derivative have been derived by Heck (2003), see also Martinec (1998) and Novák (2000), resulting in the formula

$$\frac{\partial^2 V_i(Q)}{\partial r^2} = \frac{G\rho}{r^2} \iint_{\sigma} \left[\begin{aligned} & -\frac{r'^3}{2\bar{\ell}'} + \frac{R^3}{2\bar{\ell}} + r'\bar{\ell}' - R\bar{\ell} \\ & + \frac{r'^3 \cdot (r^2 - r'^2)}{2\bar{\ell}'^3} - \frac{R^3 \cdot (r^2 - R^2)}{2\bar{\ell}^3} \\ & + 3r \cdot \cos\psi \cdot (\bar{\ell}' - \bar{\ell}) \\ & + r^2 \cdot (3\cos^2\psi - 1) \cdot \ln \left| \frac{\bar{\ell}' + r' - r \cdot \cos\psi}{\bar{\ell} + R - r \cdot \cos\psi} \right| \end{aligned} \right] \cdot d\sigma \quad (4)$$

where

$$\bar{\ell}' = \sqrt{r^2 + r'^2 - 2rr' \cdot \cos\psi}$$

$$\bar{\ell} = \sqrt{r^2 + R^2 - 2rR \cdot \cos\psi}$$

$$\cos\psi = \sin\phi \sin\phi' + \cos\phi \cos\phi' \cos(\lambda - \lambda')$$

Instead of integrating over the interval $[R, r']$ in one step, the interval can be decomposed into two parts $[R, r_p]$ and $[r_p, r']$, where r_p is the radius of the point P below Q at the intersection with the topographical surface. An elementary evaluation of the respective integrals yields the alternative formula

$$\frac{\partial^2 V_i(Q)}{\partial r^2} = \frac{8\pi G\rho}{3r^3} \cdot (r_p^3 - R^3) +$$

$$+ \frac{G\rho}{r^2} \iint_{\sigma} \left[\begin{aligned} & -\frac{r'^3}{2\bar{\ell}'} + \frac{r_p^3}{2\bar{\ell}} + r'\bar{\ell}' - r_p\bar{\ell} + \frac{r'^3 \cdot (r^2 - r'^2)}{2\bar{\ell}'^3} \\ & - \frac{r_p^3 \cdot (r^2 - r_p^2)}{2\bar{\ell}^3} + 3r \cdot \cos\psi \cdot (\bar{\ell}' - \bar{\ell}) \\ & + r^2 \cdot (3\cos^2\psi - 1) \cdot \ln \left| \frac{\bar{\ell}' + r' - r \cdot \cos\psi}{\bar{\ell} + r_p - r \cdot \cos\psi} \right| \end{aligned} \right] \cdot d\sigma \quad (5)$$

where

$$\bar{\ell}' = \sqrt{r^2 + r'^2 - 2rr' \cdot \cos\psi}$$

$$\bar{\ell} = \sqrt{r^2 + r_p^2 - 2rr_p \cdot \cos\psi}$$

The out-of-integral term in Eq. (5) can be interpreted as the effect of a spherical shell of constant density ρ and thickness $r_p - R$ on the vertical gravity gradient at Q , while the integral term corresponds to the influence of the variable terrain residual to this shell.

From an analytical point of view, the computation formulae Eqs. (4) and (5) are completely equivalent. However, the numerical properties of these formulae are quite different. Test calculations have shown that the major part of the

total topographical effect is provided by the out-of-integral term in Eq. (5), while the contribution of the integral term mostly is rather small. Thus, the integration over the spherical distance ψ may be truncated at some radius ψ_c , neglecting the far zone contribution. A straightforward application of Eq. (4) is not possible for the calculation of the contribution of the topographical column situated directly below the computation point Q, since the integrand contains terms of type 0/0 for $\psi \rightarrow 0$. Such problems do not occur in the evaluation based on Eq. (5), which therefore should be preferred in the numerical calculation of the topographical effects.

3 Generalized Condensation Model

Helmert's condensation models have been well-known in physical geodesy for more than 120 years, the first publication dating back to Helmert (1884). In his first method of condensation, Helmert proposed a redistribution of the topographical masses on an internal surface, 'parallel' to the geoid, located at a depth of 21 km below the geoid. In contrast, in the second method, the topographical masses are condensed on the geoid itself. The redistribution of masses is performed according to a local condensation procedure, i.e. a compression of the topographical column on the condensation surface. Helmert's second method of condensation has often been applied in recent years in practical geoid determination (Vaniček et al. 1999; Nahavandchi and Sjöberg 2001). A generalization of Helmert's first method in spherical approximation has been derived by Heck (2003), allowing the computation point Q to be situated outside the Earth's surface and fixing the (spherical) condensation layer at an arbitrary constant depth D below the 'geoidal sphere' Σ_g (see Figure 1). The potential of the masses condensed on the spherical surface Σ_c (radius R_c) running at the depth D below Σ_g can be expressed by the single layer potential

$$V_c(Q) = G \cdot \iint_{\sigma} \frac{\kappa'}{\ell_c} \cdot R_c^2 \cdot d\sigma, \quad (6)$$

$$\ell_c = \sqrt{r^2 + R_c^2 - 2rR_c \cdot \cos\psi}.$$

In order to fulfill the local mass conservation postulate, the surface density has to be chosen in the following way (Martinec 1998; Heck 2003)

$$\kappa' = \rho \cdot \frac{r'^3 - R^3}{3R_c^2}. \quad (7)$$

Differentiating Eq. (6) twice with respect to r yields the second radial derivative

$$\frac{\partial^2 V_c(Q)}{\partial r^2} = \frac{G\rho}{r^2} \iint_{\sigma} \left[\frac{r'^3 - R^3}{4} \cdot \left(\frac{(r^2 - R_c^2)^2}{\ell_c^5} - \frac{4r^2}{3\ell_c^3} \right) + 2 \frac{r^2 - R_c^2}{\ell_c^3} + \frac{1}{\ell_c} \right] \cdot d\sigma. \quad (8)$$

An alternative representation can be achieved by adding and subtracting the constant density $\bar{\kappa} = \kappa(\bar{P})$, where $\bar{P} \in \Sigma_c$ is situated at the intersection of the radius vector of Q (see Figure 1):

$$\frac{\partial^2 V_c(Q)}{\partial r^2} = \frac{8\pi G\rho}{3r^3} \cdot (r_p^3 - R^3) + \frac{G\rho}{r^2} \iint_{\sigma} \left[\frac{r'^3 - r_p^3}{4} \cdot \left(\frac{(r^2 - R_c^2)^2}{\ell_c^5} - \frac{4r^2}{3\ell_c^3} \right) + 2 \frac{r^2 - R_c^2}{\ell_c^3} + \frac{1}{\ell_c} \right] \cdot d\sigma. \quad (9)$$

Obviously, the out-of-integral term in Eq. (9) can be interpreted as the effect of a spherical layer with constant surface density $\bar{\kappa}$. Under the mass conservation postulate, it equals the corresponding term in Eq. (5). Thus, combining the effects of the topographical and condensation masses, the out-of-integral term cancels out in the difference between Eqs. (5) and (9), i.e.

$$\left[\frac{\partial^2 V_t(Q)}{\partial r^2} - \frac{\partial^2 V_c(Q)}{\partial r^2} \right] = \frac{G\rho}{r^2} \iint_{\sigma} \left[\begin{aligned} & -\frac{r'^3}{2\ell'} + \frac{r_p^3}{2\ell} + r'\bar{\ell}' - r_p\bar{\ell} + \frac{r'^3 \cdot (r^2 - r'^2)}{2\ell'^3} \\ & - \frac{r_p^3 \cdot (r^2 - r_p^2)}{2\ell^3} + 3r \cdot \cos\psi \cdot (\bar{\ell}' - \bar{\ell}) \\ & + r^2 \cdot (3\cos^2\psi - 1) \cdot \ln \left| \frac{\bar{\ell}' + r' - r \cdot \cos\psi}{\bar{\ell} + r_p - r \cdot \cos\psi} \right| \\ & - \frac{r'^3 - r_p^3}{4} \cdot \left(\frac{(r^2 - R_c^2)^2}{\ell_c^5} - \frac{4r^2}{3\ell_c^3} \right) \\ & + 2 \frac{r^2 - R_c^2}{\ell_c^3} + \frac{1}{\ell_c} \end{aligned} \right] \cdot d\sigma \quad (10)$$

It should be noted that – after a suitable choice of the depth D of the condensation level – the results of the extended Helmert condensation model are

practically equivalent to the Airy-Heiskanen model; a detailed proof will be given in a forthcoming paper. The advantage of Helmert's model relies on the fact that only two-dimensional instead of three-dimensional integrals have to be evaluated.

4 Results

In order to investigate the properties of the derived procedure, a simulation based on the JGP95E digital elevation model (Lemoine et al. 1998) has been performed, involving a $1^\circ \times 1^\circ$ grid of rock-equivalent topography. The radii of the mean Earth sphere (R), the concentric spheres of condensation (R_c) and the satellite (r) have been chosen in the following way:

$$\begin{aligned} R &= 6371 \text{ km} \\ R_c &= \begin{cases} R - 21 \text{ km} = 6350 \text{ km} & \text{(Helmert I)} \\ R - 0 \text{ km} = 6371 \text{ km} & \text{(Helmert II)} \end{cases} \\ r &= R + 260 \text{ km} = 6631 \text{ km} \quad (\text{GOCE-like orbit}). \end{aligned}$$

In the numerical evaluation, the integration over any spherical $1^\circ \times 1^\circ$ cell $\Delta\sigma_i$ has been replaced by summation

$$\iint_{\Delta\sigma_i} f(r, r', \psi) \cdot d\sigma \approx f(r, r'_m, \psi_m) \cdot \Delta\sigma_i,$$

where r'_m, ψ_m refer to the centre of the cell $\Delta\sigma_i$.

In a first test, the equivalence of the numerical results based on the pair of equations (4), (8) versus the set (5), (9) has been proved. In the sequel, Eqs. (5), (9) and (10) have been applied in the numerical calculations for the reasons discussed at the end of section 2. Furthermore, both Helmert I and II models have been compared.

The second radial derivative $\partial^2 V_t / \partial r^2$ of the topographic potential at the satellite height is illustrated in Figure 2. Maxima are visible in high-mountain regions, while minima occur near the deep-sea troughs. The total range of the signal is at the 10 E.U. level. At first sight, the results for the second radial derivative $\partial^2 V_c / \partial r^2$ of the condensation potential, corresponding to the Helmert I and II models, are practically the same and cannot be distinguished from Figure 2; the corresponding figures are not shown here.

The combined topographic-condensation effects for Helmert's first and second models are illustrated in Figures 3 and 4. It is obvious that both constituents partly cancel each other, such that the complete topographic-isostatic reduction of gravity gradients is one order of magnitude less in

comparison to the single constituents in the case of the Helmert I model.

This cancellation property is even more pronounced for the Helmert II model (see Figure 4). The total topographic-isostatic reduction term is more than two orders of magnitude smaller than the single constituents.

Considering the fact that the isostatic masses compensating the Earth's topography are situated at a depth of about 20-30 km below sea level it is evident that Helmert's first model is a much better approximation to geophysical reality (Heck 2002). Thus, it becomes obvious that the topographic-isostatic reduction of gravity gradients is strongly underestimated when the reduction is calculated on the basis of Helmert's second model. As a consequence, the residual gravity gradient field – after having applied topographic-condensation reduction – will be much rougher when Helmert's second model is applied in the remove-restore process, and downward continuation is much more problematic.

5 Conclusions

It has become evident that topographic and isostatic effects are significant in satellite gradiometry, showing an order of magnitude of 10 E.U. in the second vertical derivatives of the potentials V_t and V_c at a satellite altitude of 260 km (approximately GOCE orbit). Topographic and isostatic effects corresponding to Helmert's first and second condensation models cancel out at a large extent. The combined effect amounts to about 0.6 E.U. for Helmert's first model, and 0.06 E.U. for Helmert's second model. Since Helmert's second model produces too low topographic-isostatic reduction terms, the residual field after having applied topographic-condensation reduction will remain rather rough; thus downward continuation of this field will be problematic.

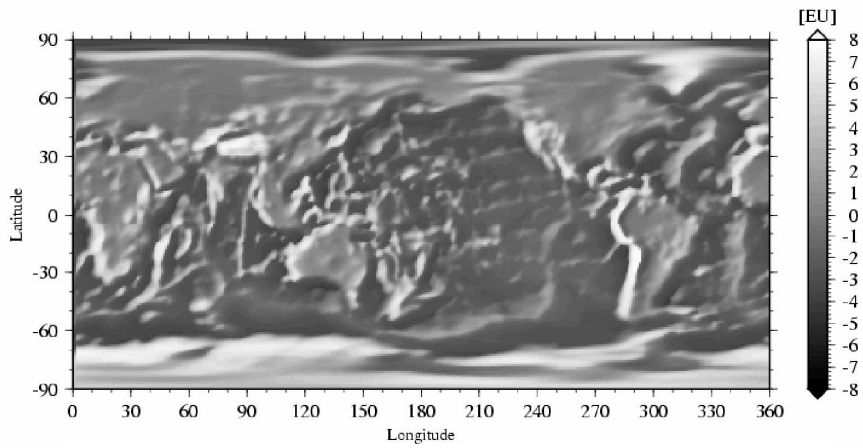


Figure 2. Second radial derivative $\partial^2 v_t / \partial r^2$ (nearly identical with $\partial^2 v_c / \partial r^2$)

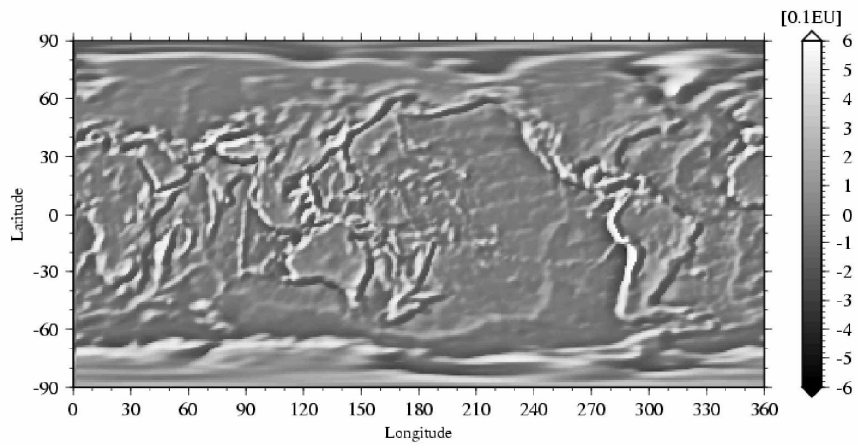


Figure 3. Topographic-condensation reduction $\left[\partial^2 v_t / \partial r^2 - \partial^2 v_c / \partial r^2 \right]$ for the Helmert I model

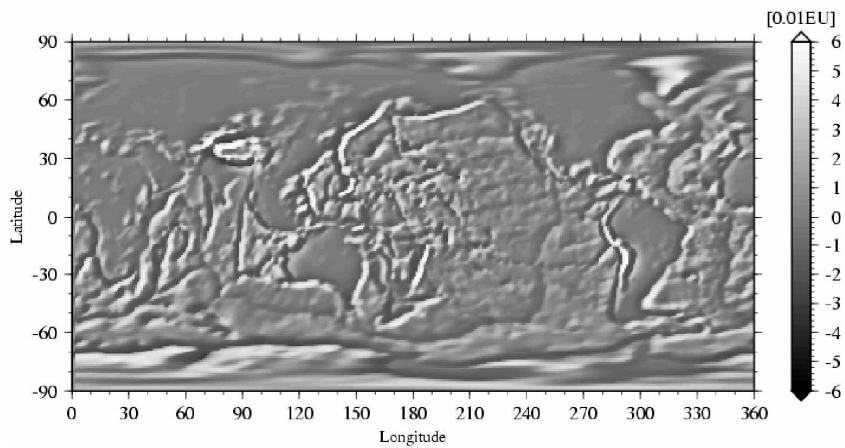


Figure 4. Topographic-condensation reduction $\left[\partial^2 v_t / \partial r^2 - \partial^2 v_c / \partial r^2 \right]$ for the Helmert II model

Appendix A

In Heck (2003) the following identity has been derived:

$$\frac{\partial}{\partial r} \left(\frac{\xi^2}{\ell} \right) = \frac{2}{r} \cdot \frac{\xi^2}{\ell} - \frac{\partial}{\partial \xi} \left(\frac{\xi^3}{r\ell} \right), \ell = \sqrt{r^2 + \xi^2 - 2r\xi \cdot \cos \psi}. \quad (A1)$$

A second differentiation with respect to r and elementary transformation of the right hand side yields

$$\begin{aligned} \frac{\partial^2}{\partial r^2} \left(\frac{\xi^2}{\ell} \right) &= \frac{2}{r} \cdot \frac{\partial}{\partial r} \left(\frac{\xi^2}{\ell} \right) - \frac{2}{r^2} \left(\frac{\xi^2}{\ell} \right) + \\ &+ \frac{\partial}{\partial \xi} \left(\frac{3\xi^3}{2r^2\ell} + \frac{\xi^3(r^2 - \xi^2)}{2r^2\ell^3} \right). \end{aligned} \quad (A2)$$

This relationship can be used for deriving an analytical expression for the second radial derivative of the Newton integral (1):

$$\begin{aligned} \frac{\partial^2 V_t(Q)}{\partial r^2} &= G \cdot \rho \cdot \iint_{\sigma[R]} \left[\frac{r'}{r} \cdot \frac{\partial^2}{\partial r^2} \left(\frac{\xi^2}{\ell} \right) \right] \cdot d\sigma \\ &= G \cdot \rho \cdot \iint_{\sigma[R]} \left[\frac{r'}{r} \cdot \left(\frac{2}{r} \cdot \frac{\partial}{\partial r} \left(\frac{\xi^2}{\ell} \right) - \frac{2}{r^2} \left(\frac{\xi^2}{\ell} \right) + \right. \right. \\ &\quad \left. \left. + \frac{\partial}{\partial \xi} \left(\frac{3\xi^3}{2r^2\ell} + \frac{\xi^3(r^2 - \xi^2)}{2r^2\ell^3} \right) \right) \right] \cdot d\xi \cdot d\sigma \\ &= \frac{2}{r} \cdot \frac{\partial V_t(Q)}{\partial r} - \frac{2}{r^2} \cdot V_t(Q) + \frac{G \cdot \rho}{2 \cdot r^2} \iint_{\sigma[R]} \left[\frac{3\xi^3}{\ell} + \frac{\xi^3 \cdot (r^2 - \xi^2)}{\ell^3} \right] \Big|_{\xi=R}^{\xi=r'} \cdot d\sigma \end{aligned}$$

Acknowledgements: The authors gratefully acknowledge the valuable comments by W. Featherstone und D. Tsoulis.

References

- Heck B (2002) On the use and abuse of Helmert's second method of condensation. In: Ádám J, Schwarz KP (eds) *Vistas for Geodesy in the new millennium*. Springer IAG Symposia, Vol. 125
- Heck B (2003) On Helmert's methods of condensation. *Journal of Geodesy* 77: 155-170
- Helmert FR (1884) *Die mathematischen und physikalischen Theorien der Höheren Geodäsie*. II. Teil: Die physikalischen Theorien, B.G. Teubner, Leipzig (reprinted 1962)
- Kuhn M (2003) Geoid determination with density hypothesis from isostatic models and geological information. *Journal of Geodesy* 77: 50-65
- Lemoine FG, Kenyon SC, Factor JK, Trimmer R, Pavlis NK, Chinn DS, Cox CM, Klosko SM, Luthcke SB, Torrence

MH, Wang YM, Williamson RG, Pavlis EC, Rapp RH, Olson TR (1998) The development of the NASA GSFC and National Imaginary and Mapping Agency (NIMA) geopotential model EGM96. Rep. NASA/TP-1998-206861, National Aeronautics and Space Administration, Maryland

Martinec Z (1998) Boundary-value problems for gravimetric determination of a precise geoid. Lecture notes in Earth Sciences 73. Springer, Berlin Heidelberg New York

Nahavandchi H, Sjöberg LE (2001) Precise geoid determination over Sweden using the Stokes-Helmert method and improved topographic corrections. *Journal of Geodesy* 75: 74-88

Novák P (2000) Evaluation of gravity data for the Stokes-Helmert solution to the geodetic boundary value problem. PhD Dissertation, Techn. Rep. of the Dept. of Geodesy and Geomatics Engineering, 207, University of New Brunswick, Fredericton

Tsoulis D (1999) Analytical and numerical methods in gravity field modelling of ideal and real masses. Deutsche Geodätische Kommission, C 510, Munich

Vanicek P, Huang J, Pagiatakis S, Véronneau M, Martinec Z, Featherstone W (1999) Determination of boundary values for the Stokes-Helmert problem. *Journal of Geodesy* 73: 180-192